  Bull. Chem. Soc. Jpn., 56, 991—996 (1983)

A Potential-step Chronoamperometric Study of Ion Transfer at the Water/Nitrobenzene Interface

Tadaaki KAKUTANI, Toshiyuki OSAKAI, and Mitsugi SENDA*

Department of Agricultural Chemistry, Faculty of Agriculture, Kyoto University, Kyoto 606

(Received August 2, 1982)

Potential-step chronoamperometry, cyclic voltammetry, and chronopotentiometry have been applied to the study of the transfer of the tetramethylammonium (TMA^+) ion across the interface between a 0.1 mol dm^{-3} lithium chloride aqueous solution and a 0.1 mol dm^{-3} tetrabutylammonium tetraphenylborate nitrobenzene solution. An analysis of the current-time and current-potential curves obtained by means of potential-step chronoamperometry indicates that the transfer of the TMA^+ ion across the water/nitrobenzene interface is a reversible diffusion-controlled process, which can be explained by the theory of the chronoamperometry of a reversible charge transfer at the electrode surface. The values of the diffusion coefficient of the TMA^+ ion in the aqueous phase and of the reversible half-wave potential of the TMA^+ ion transfer, as determined by means of potential-step chronoamperometry, agreed well with those determined by means of cyclic voltammetry and chronopotentiometry.

Recently there has been growing interest in electrochemical phenomena occurring at the interface between oil and water or two immiscible liquids (for reviews, see Refs. 1, 2, and 3). Electrochemical information on the charge (ion or electron) transfer at the liquid-liquid interface is important for a better understanding of the solvent extraction of ions, of liquid membrane ion-selective electrodes, and of the biological membrane and its model systems. Although several electrochemical techniques have been developed for studying the ion transfer at the interface between two immiscible electrolyte solutions (chronopotentiometry with the stationary interface,[4] cyclic voltammetry with the stationary interface,[5,6] and d.c. polarography with the electrolyte dropping electrode[7-9]), the further development of experimental approaches to the electrochemistry of the ion transfer at the interface seems highly desirable. In this work we have applied potential-step chronoamperometry to the study of the tetramethylammonium (TMA^+) ion transfer at the stationary water/nitrobenzene interface. The electrochemical data obtained by this techniques were then compared with those obtained by cyclic voltammetry and chronopotentiometry.

Experimental

Chemicals. The tetrabutylammonium tetraphenylborate (TBATPB) was prepared by the equimolar addition of an aqueous solution of tetrabutylammonium bromide to an aqueous solution of sodium tetraphenylborate and purified by repeated recrystalizations from acetone. The lithium chloride was a Merck product of the "spurapur" grade. The tetramethylammonium bromide (TMABr) and tetrabutylammonium chloride (TBACl) were analytical reagent-grade products of the Nakarai Chemicals Co. These reagents were used as received. Analytical-grade nitrobenzene was shaken with neutral alumina overnight; after the filtration of the suspension, the filtrate was fractionally distilled under a vacuum. The central 60% fraction of the distillate was collected and washed with triply distilled water. Triply distilled water was also used to prepare the aqueous electrolyte solutions.

Electrochemical Measurements. The transfer of the TMA^+ ion across the interface between a 0.1 mol dm^{-3} TBATPB nitrobenzene solution (Phase II in Cell A) and a 0.1 mol dm^{-3} LiCl aqueous solution containing $(0.5—2)\times10^{-3}$ mol dm^{-3} TMABr (Phase III in Cell A) was studied. The electrolytic cell assembly is shown in Fig. 1. The test interface, *i.e.*, the water/nitrobenzene interface to be studied for the transfer of the TMA^+ ion, is formed in a glass tube A. A flat and reproducible water/nitrobenzene interface, with an area of 0.159 cm^2, can be formed by treating with dimethyldichlorosilane the inner surface of the tube A that will come in contact with nitrobenzene.[10] The potential difference across the test interface was controlled by a four-electrode potentiostat,[5,10] with two reference electrodes and two counter electrodes. The reference electrode for the nitrobenzene phase, RE2, was an Ag/AgCl/0.1 mol dm^{-3} TBACl (water) electrode which was connected to the nitrobenzene phase by means of a Luggin capillary filled with the 0.1 mol dm^{-3} TBATPB nitrobenzene solution. The reference electrode for the aqueous phase, RE1, was an Ag/AgCl electrode immersed in an aqueous phase containing 0.1 mol dm^{-3} LiCl. Accordingly, the cell to be studied can be expressed by:

$$\begin{array}{l}\overset{\text{I}}{\text{(RE2) Ag|AgCl|0.1 mol dm}^{-3}\text{ TBACl(W)}}\\ \overset{\text{II}}{\text{|0.1 mol dm}^{-3}\text{TBATPB(N)}}\\ \left|\begin{array}{l}\overset{\text{III}}{(0.5-2)\times10^{-3}\text{ mol dm}^{-3}\text{ TMABr}}\\ \qquad\qquad\qquad\qquad\text{(W)}\\ \qquad+\text{ 0.1 mol dm}^{-3}\text{ LiCl}\end{array}\right.\\ \overset{\text{IV}}{\text{|0.1 mol dm}^{-3}\text{ LiCl(W)|AgCl|Ag(RE1).}}\end{array}\quad\text{(A)}$$

As the counter electrodes, Ag/AgCl electrodes with a large surface area (>4 cm^2) were used. One of the counter electrodes, CE1, was immersed in the aqueous phase, while the other, CE2, was immersed in a 0.1 mol dm^{-3} TBACl aqueous solution which was connected to the nitrobenzene phase through sintered glass. The location of the tip of the Luggin capillary of the reference electrode was adjusted by using a manipulator, Narishige BC-4; the distance, d_W, between the tip of the Luggin capillary of RE1 and the test interface, and the distance, d_N, between the tip of the Luggin capillary of RE2 and the test interface, were accurately measured by means of a travelling microscope, PIKA Seiko Co., Model PRM-2XYZ. Usually d_N and d_W were set at 0.2 mm and 1.0 mm respectively. Then the resistance of the electrolyte-solution column between the tips of the two Luggin capillaries, RE1 and RE2, r_s, was estimated to be 180 Ω, as calculated from the conductivities of the electrolyte solutions and the area of the test interface. The conductivities of the 0.1 mol dm^{-3} LiCl aqueous solution and the 0.1 mol dm^{-3} TBATPB nitrobenzene solution were

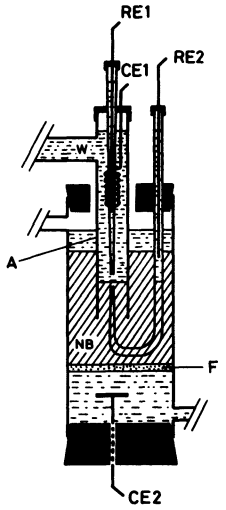

Fig. 1. Electrolytic cell. W: Water phase; NB: nitrobenzene phase; A: glass tube; REl and RE2: reference electrodes; CEl and CE2: counter electrodes; F: sintered glass.

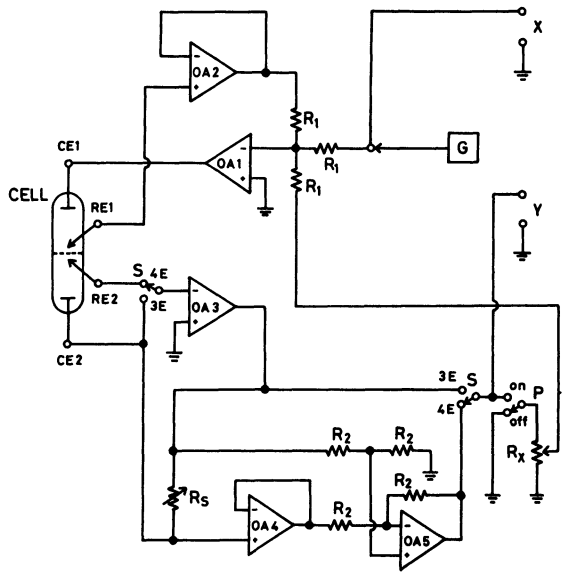

Fig. 2. Electronic circuit of the four-electrode potentiostat with the cell system. G: Sweep and step function generator; X and Y: X- and Y-axis inputs of recorder; RE1 and RE2: reference electrodes; CE1 and CE2: counter electrodes; OA1 to OA5: operational amplifiers, Burr Brown 3112/12C; R_s: current-measuring resistor, variable; R_1 and R_2: resistor, 10 kΩ; S: switch, in position 4E for the four-electrode potentiostat operation and in position 3E for the three-electrode potentiostat operation; P: switch, in on position for positive feedback for iR compensation; R_x: resistor for positive feedback, adjustable.

determined to be 9.48×10^{-3} and 1.12×10^{-3} Ω^{-1} cm^{-1} respectively at 25 °C.

For potential-step chronoamperometry and cyclic voltammetry, a four-electrode potentiostat,[10] to which a Yanako Model PE21-TB2S potentiostat was remodelled, and a function generator, Nikko Keisoku Model NFG-3, were used. Figure 2 shows the basic electronic circuit of the four-electrode potentiostat, with the cell system. The current-time curves of the potential-step chronoamperometry were recorded using both a transient memory, Union Giken System 71-02, and an X–Y recorder, Yokogawa 3077. The cyclic voltammograms were recorded with the same X–Y recorder. For chronopotentiometry, the current across the two counter electrodes (CEl and CE2) of the cell in Fig. 1 was controlled using a conventional, laboratory-made galvanostat,[10,14] and the potential difference across the test interface was measured by means of the two reference electrodes (REl and RE2), using a laboratory-made, high-input-impedance differential amplifier and an X–Y recorder, Yokogawa 3077. All the electrochemical measurements were performed at 25±2 °C.

Results

In the following remarks, the potential applied to the cell A, E, is defined as the potential difference between the two reference electrodes, REl and RE2, *i.e.*, $E=E_{RE1}-E_{RE2}$. The flow of the positive charge from the aqueous to the nitrobenzene phase is considered as the positive current.

Potential-step Chronoamperometry. In this method, a potential step $\Delta E=E-E_i$, E_i being the initial potential where the current due to the ion transfer is negligible, is applied to the test interface at time $t=0$, and the resulting current, i, is recorded against t. For studying the TMA^+ ion transfer from the aqueous to the nitrobenzene phase, E_i was set at 200 mV. Figure 3 shows an example of the current-time curves of the TMA^+-ion transfer from the aqueous to the nitrobenzene phase. The currents measured at various E's, when corrected for the base current, were inversely proportional to $t^{1/2}$ at $t>0.1$ s, as is shown in Fig. 4. This indicates that the transfer of the TMA^+ ion from the aqueous to the nitrobenzene phase is a diffusion-controlled process at $t>0.1$ s. Figure 5 shows a plot of the current measured at $t=10$ s, $I_{t=10\,s}$, against

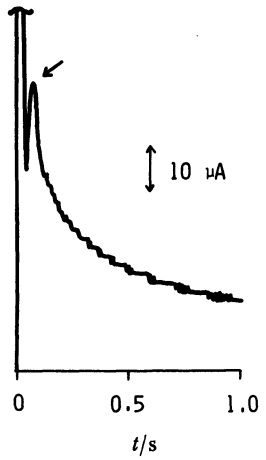

Fig. 3. Chronoamperometric current-time(i-t) curve of TMA^+ ion transfer from the aqueous to the nitrobenzene phase at $E=0.38$ V for 0.5×10^{-3} TMA^+ in 0.1 mol dm^{-3} LiCl aqueous solution. A transient oscillation of the current (as indicated by an arrow) was sometimes observed, depending on the solution resistance and ion transfer impedance at the interface, at the initial part of i-t record.

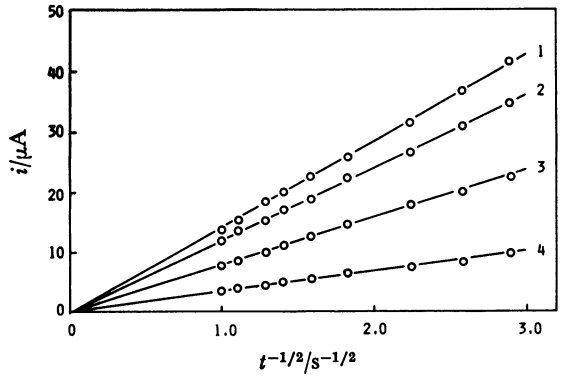

Fig. 4. Plots of i, corrected for the base current, against $t^{-1/2}$ for 0.5×10^{-3} mol dm^{-3} TMA$^+$ ion in 0.1 mol dm^{-3} LiCl aqueous solution. E: (1) 0.38, (2) 0.35, (3) 0.32, (4) 0.29 V.

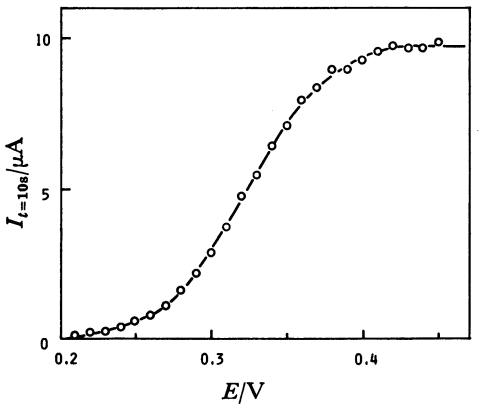

Fig. 5. Plot of $I_{t=10s}$, corrected for the base current, against E for 1×10^{-3} mol dm^{-3} TMA$^+$ ion in 0.1 mol dm^{-3} LiCl aqueous solution.

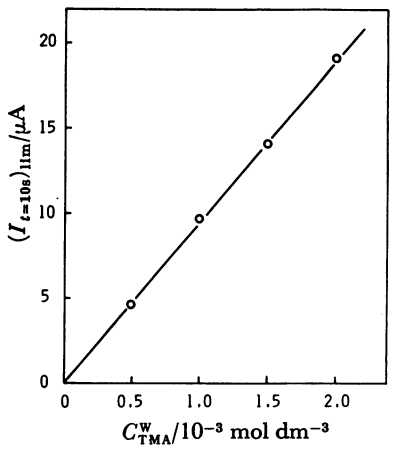

Fig. 6. Dependence of limiting current, $(I_{t=10s})_{lim}$, on the bulk concentration of TMA$^+$ ion, C^W_{TMA}, in 0.1 mol dm^{-3} LiCl aqueous solution.

E for 10^{-3} mol dm^{-3} TMABr in a 0.1 mol dm^{-3} LiCl aqueous solution; it gives a well-defined current-potential ($I_{t=10s}-E$) curve, with the limiting current, $(I_{t=10s})_{lim}$, and the half-wave potential, $E_{1/2}$, for the transfer of the TMA$^+$ ion from the aqueous to the nitrobenzene phase. In the present case (d_N=0.2 mm,

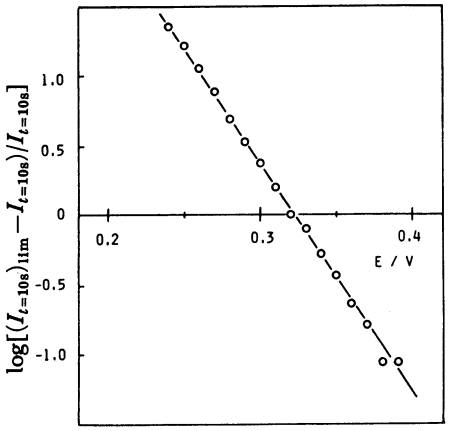

Fig. 7. Logarithmic analysis of the current-potential ($I_{t=10s}-E$) curve shown in Fig. 5.

d_w=1.0 mm, and t=10 s), the ohmic drop due to r_s was estimated to be always less than 4 mV, even for the 2.0×10^{-3} mol dm^{-3} TMA$^+$ ion in the aqueous phase. Accordingly, no correction for the ohmic drop was made. The limiting current was proportional to the bulk concentration of the TMA$^+$ ion in the aqueous phase, as is shown in Fig. 6. Figure 7 shows a logarithmic analysis of the wave, giving a straight line with the slope of 60 mV. The half-wave potential was 0.32 V, independently of the bulk concentration of the TMA$^+$ ion. These results indicate that the $I_{t=10s}-E$ curve of the TMA$^+$ ion transfer has the same characteristics as a reversible d.c. polarographic wave:

$$E = E^r_{1/2,j} + (RT/z_jF)\ln[I_{t=t_s}/((I_{t=t_s})_{lim} - I_{t=t_s})], \quad (1)$$

where $E^r_{1/2,j}$ is the reversible half-wave potential of the j ion (here, j=TMA$^+$); z_j the ionic valence of the j ion, and $I_{t=t_s}$, the ion-transfer current at $t=t_s$ (here, t_s=10 s).

The limiting current at $t=t_s$, $(I_{t=t_s})_{lim}$, due to the diffusion-controlled j ion transfer from the aqueous to the nitrobenzene phase should be given by the Cottrell equation:[11]

$$(I_{t=t_s})_{lim} = z_jFA(D^W_j/\pi t_s)^{1/2}C^W_j, \quad (2)$$

where A is the surface area; C^W_j, the bulk concentration, and D^W_j the diffusion coefficient of the j ion in the aqueous phase (W). The application of this equation to the plot in Fig. 6 yielded the diffusion coefficient of the TMA$^+$ ion in the aqueous phase, D^W_{TMA}. The values of $E^r_{1/2,TMA}$ and D^W_{TMA} as determined by means of potential-step chronoamperometry are summarized in Table 1.

Cyclic Voltammetry. Figure 8 shows cyclic voltammograms of the 2×10^{-3} mol dm^{-3} TMA$^+$ ion in the aqueous phase. The positive-current peak on the forward polarization and the negative-current peak on the following backward polarization correspond, respectively, to the transfer of the TMA$^+$ ion from the aqueous to the nitrobenzene phase and its transfer back to the aqueous phase. The voltammograms were influenced by the solution resistance, r_s. The peak potentials of the positive and negative currents, E_{pa} and E_{pc}, varied linearly with d_N, as is shown in Fig. 9.[10] The slopes of

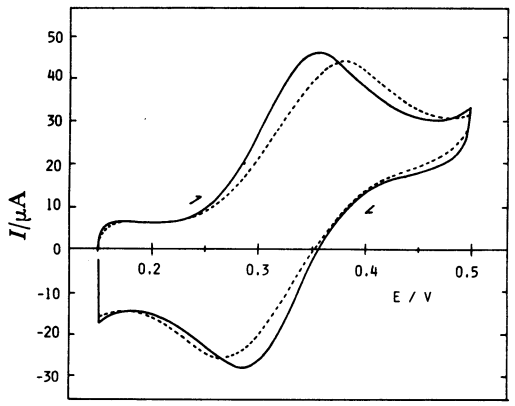

Fig. 8. Cyclic voltammograms for the transfer of 2×10^{-3} mol dm^{-3} TMA^+ ion from 0.1 mol dm^{-3} LiCl aqueous solution to 0.1 mol dm^{-3} TBATPB nitrobenzene solution and back at $v=20$ mV s^{-1}. Solid line: measured at $d_N=0.2$ mm and $d_W=1.0$ mm. Dotted line: measured at $d_N=d_W=1.0$ mm.

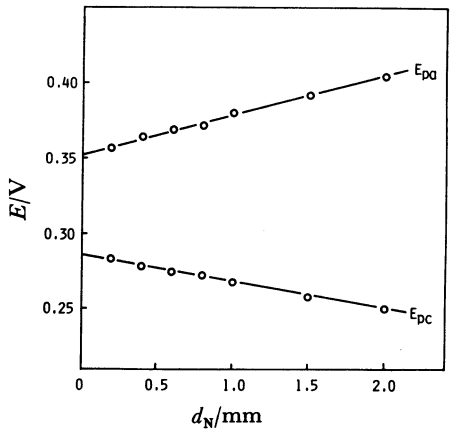

Fig. 9. Plots of the peak potentials of the positive and negative current, E_{pa} and E_{pc}, against d_N for 2×10^{-3} mol dm^{-3} TMA^+ ion in 0.1 mol dm^{-3} LiCl aqueous solution. d_W: 1.0 mm; v: 20 mV s^{-1}.

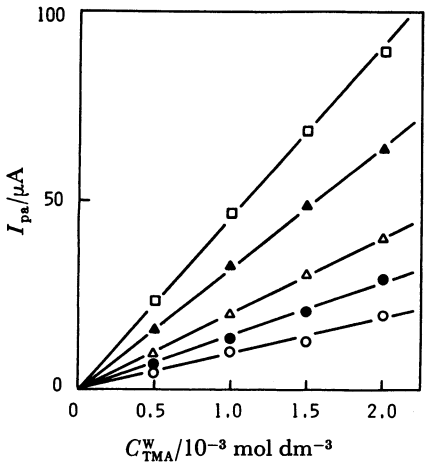

Fig. 10. Dependence of the positive peak current of cyclic voltammogram of TMA^+ ion transfer, I_{pa}, on the bulk concentration of TMA^+ ion, C^W_{TMA}, in 0.1 mol dm^{-3} LiCl aqueous solution. v: (○) 5, (●) 10, (△) 20, (▲) 50, and (□) 100 mV s^{-1}.

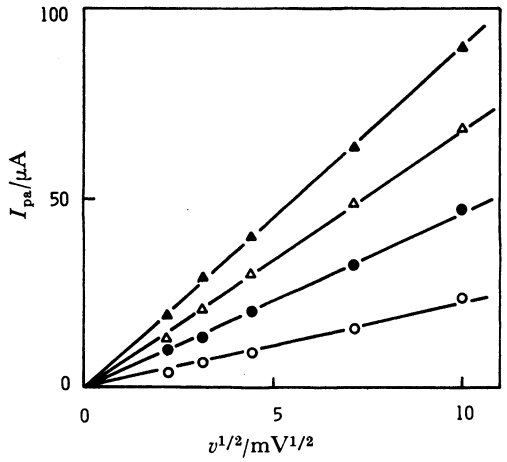

Fig. 11. Dependence of the positive peak current of cyclic voltammogram of TMA^+ ion transfer, I_{pa}, on the voltage scan rate, v. C^W_{TMA}: (○) 0.5×10^{-3}, (●) 1.0×10^{-3}, (△) 1.5×10^{-3}, and (▲) 2.0×10^{-3} mol dm^{-3}.

the linear plots gave 636 Ω mm^{-1} (average of these two plots) for the resistance per mm of the nitrobenzene-solution column; this value agreed well with the calculated value of 563 Ω mm^{-1}. The extrapolation of E_{pa} and E_{pc} to $d_N=0$ should yield the peak potentials corrected for the ohmic drop in the nitrobenzene phase. Correction for the ohmic drop in the nitrobenzene as well as the aqueous phase yielded the corrected peak potentials, $E_{pa,corr}$ and $E_{pc,corr}$, which were independent of both the concentration of the TMA^+ ion in the aqueous phase, C^W_{TMA}, in the range between 0.5×10^{-3} and 2×10^{-3} mol dm^{-3} and the scan rate, v, in the range between 5 and 100 mV s^{-1}. The corrected peak separations, $\Delta E_{p,corr}=E_{pa,corr}-E_{pc,corr}$, were 60 mV over the scan-rate range of 5 to 100 mV s^{-1} for all the concentration of the TMA^+ examined. When $r_s=180$ Ω ($d_N=0.2$ mm and $d_w=1.0$ mm), the positive peak current, I_{pa}, was proportional to the concentration of the TMA^+ ion and to the square root of the voltage-scan rate (see Figs. 10 and 11). Similarly, the negative peak current, I_{pa}, was proportional to the concentration of the TMA^+ ion in the aqueous phase and to the square root of the voltage-scan rate (data are not shown). These results indicated that the transfer of the TMA^+ ion across the water/nitrobenzene interface was a diffusion-controlled process over the scan-rate range from 5 to 100 mV s^{-1}. Accordingly, the theory of the voltammetry of a reversible charge transfer at the electrode surface[11] was used to analyse the cyclic voltammetric data. The reversible half-wave potential (or the midpoint potential between $E_{pa,corr}$ and $E_{pc,corr}$) and the diffusion coefficient of the TMA^+ ion in the aqueous phase, as determined by cyclic voltammetry, are given in Table 1.

Chronopotentiometry. Figure 12 shows chronopotentiometric potential-time ($E-t$) curves with the current reversal at various current densities for the transfer of the TMA^+ ion from the aqueous to the nitrobenzene phase and its transfer back to the aqueous phase. The transition times were inversely proportional to the square of the current density over the range from

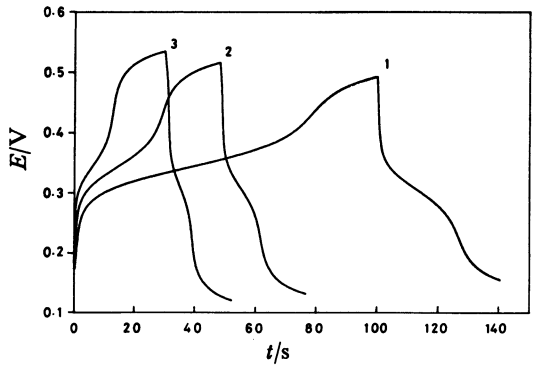

Fig. 12. Chronopotentiometric potential-time curves with current reversal for TMA^+ ion transfer across the water/nireobenzene interface for 1×10^{-3} mol dm^{-3} TMA^+ ion in 0.1 mol dm^{-3} LiCl aqueous solution. The current density: (1) 31.4, (2) 62.9, and (3) 94.3 μA cm^{-2}.

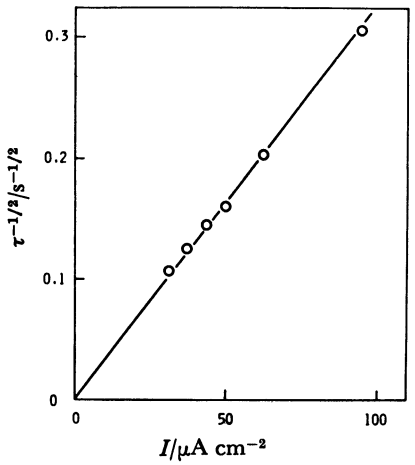

Fig. 13. Dependence of the chronopotentiometric transition time of TMA^+ ion transfer from the aqueous to the nitrobenzene phase, τ, on the current density, I, for the transfer of 1×10^{-3} mol dm^{-3} TMA^+ ion from 0.1 mol dm^{-3} LiCl aqueous solution to 0.1 mol dm^{-3} TBATPB nitrobenzene solution.

TABLE 1. HALF-WAVE POTENTIAL FOR THE TRANSFER OF TMA^+ ION ACROSS WATER/NITROBENZENE INTERFACE AND DIFFUSION COEFFICIENT OF TMA^+ ION IN THE AQUEOUS PHASE AS DETERMINED BY THREE ELECTROCHEMICAL METHODS

Method	$E^r_{1/2,TMA}$ / V	D^w_{TMA} / 10^{-5} cm^2 s^{-1}
Potential-step chrononoamperometry	0.32	1.2
Cyclic voltammetry	0.32	1.1
Chronopotentiometry	0.32	1.3

31.4 to 94.3 μA cm^{-2} (Fig. 13). Thus, the chronopotentiometric behavior was interpreted by means of the theory of the chronopotentiometry of a reversible charge transfer at the electrode surface.[11] The reversible half-wave potential and the diffusion coefficient of the TMA^+ ion in the aqueous phase, as determined from the chronopotentiometric data, are given in Table 1.

All three methods yielded the same values of the half-wave potential for the transfer of the TMA^+ ion across the water/nitrobenzene interface and of the diffusion coefficient of the TMA^+ ion in the aqueous phase.

Discussion

We shall define the standard ion-transfer potential of the j ion across the water(W)/nitrobenzene(N) interface, $\Delta^w_N\phi^\ominus_j$, by:

$$\Delta^w_N\phi^\ominus_j = -\Delta G^{\ominus,N\to W}_{tr,j}/z_jF, \quad (3)$$

where $\Delta G^{\ominus,N\to W}_{tr,j}$ is the standard Gibbs free energy of the transfer of the j ion from the nitrobenzene to the aqueous phase. Then, $E^r_{1/2,j}$ is given by:

$$E^r_{1/2,j} = \Delta^w_N\phi_{1/2,j} + \Delta E_{ref}, \quad (4)$$

$$\Delta^w_N\phi_{1/2,j} = \Delta^w_N\phi^\ominus_j + (RT/z_jF)\ln(\gamma^N_j\sqrt{D^w_j}/\gamma^w_j\sqrt{D^N_j}), \quad (5)$$

where ΔE_{ref} is the constant which depends only on the reference electrode system, and where γ^N_j and γ^w_j are the activity coefficients of the j ion in the nitrobenzene and aqueous phases respectively. For the reference electrodes, RE1 and RE2, used here, ΔE_{ref} in Eq. 4 is given by:

$$\Delta E_{ref} = -\Delta\phi_L + E_{Ag/AgCl/0.1\ mol\ dm^{-3}\ LiCl(W)} - E_{Ag/AgCl/0.1 mol\ dm^{-3}\ TBACl(W)}, \quad (6)$$

where $\Delta\phi_L(=\phi^w_I-\phi^N_{II})$ is the potential difference between a 0.1 mol dm^{-3} TBACl aqueous solution(I) and a 0.1 mol dm^{-3} TBATPB nitrobenzene solution(II). Since $\Delta^w_N\phi^\ominus_{TPB}$ is extremely positive compared with $\Delta^w_N\phi^\ominus_{TBA}$, while $\Delta^w_N\phi^\ominus_{Cl}$ is extremely negative compared with $\Delta^w_N\phi^\ominus_{TBA}$, $\Delta\phi_L$ is given in a good approximation by:[10,12]

$$\Delta\phi_L = \Delta^w_N\phi^\ominus_{TBA} + (RT/F)\ln(\gamma^N_{TBA}C^N_{TBA}/\gamma^w_{TBA}C^w_{TBA}), \quad (7)$$

where γ^α_{TBA} and C^α_{TBA} (α=N and W) are the activity coefficient and the concentration of the TBA^+ ion respectively in the nitrobenzene(N) and aqueous(W) phases. The validity of Eq. 7 for the interface between the 0.1 mol dm^{-3} TBACl aqueous solution and the 0.1 mol dm^{-3} TBATPB nitrobenzene solution was proved by measuring the electromotive force, E_{emf}, of the following cell:

$$\begin{array}{l} \overset{I}{Ag|AgCl|0.1\ mol\ dm^{-3}TBACl(W)} \\ \overset{II}{|0.1\ mol\ dm^{-3}\ TBATPB(N)|} \\ \left|\begin{array}{l} \overset{III}{x\ mol\ dm^{-3}\ TBACl} \\ (0.1-x) mol\ dm^{-3}\ LiCl \end{array}\right. (W) \left| AgCl \right| Ag \end{array} \quad (B)$$

for 0.02 mol dm^{-3} $\leq x\leq$ 0.1 mol dm^{-3}; E_{emf} depended linearly on $\ln(C^{III}_{TBA}/C^{I}_{TBA})$, with a slope of 26 mV ($=RT/F$).[10] Upon assuming that $E_{Ag/AgCl/0.1\ mol\ dm^{-3}\ LiCl(W)} - E_{Ag/AgCl/0.1\ mol\ dm^{-3}\ TBACl(W)} \approx 0$, we obtain:

$$\begin{aligned} E^r_{1/2,TBA} &= \Delta^w_N\phi^\ominus_{TMA} + (RT/F)\ln(\gamma^N_{TMA}\sqrt{D^w_{TMA}}/\gamma^w_{TMA}\sqrt{D^N_{TMA}}) \\ &\quad - \Delta^w_N\phi^\ominus_{TBA} - (RT/F)\ln(\gamma^N_{TBA}C^N_{TBA}/\gamma^w_{TBA}C^w_{TBA}) \quad (8) \\ &\approx \Delta^w_N\phi^\ominus_{TMA} - \Delta^w_N\phi^\ominus_{TBA} + (RT/F)\ln(\sqrt{D^w_{TMA}}/\sqrt{D^N_{TMA}}) \end{aligned}$$

since $C^N_{TBA}=C^w_{TBA}=0.1$ mol dm^{-3}, and $\ln(\gamma^N_{TMA}\gamma^w_{TBA}/\gamma^w_{TMA}\gamma^N_{TBA})\approx 0$. The standard ion-transfer potentials of the TMA^+ and TBA^+ ions, as estimated from the ionic distribution coefficient data, are given[13] as $\Delta^w_N\phi^\ominus_{TMA} - \Delta^w_N\phi^\ominus_{TBA} = 0.283$ V, which is 40 mV more negative than

the present result of $E^{r}_{1/2,TMA}=0.32$ V. This difference cannot be explained by the $(RT/F)\ln(\sqrt{D}^{W}_{TMA}/\sqrt{D}^{N}_{TMA})$ terms. It seems premature to discuss the origin of this discrepancy.

The potential-step chronoamperometry appears a promising technique for the investigation of the charge-transfer processes at the interface between two immiscible electrolyte solutions.

References

1) A. Watanabe and H. Tamai, *Hyomen*, **13**, 67 (1975).
2) J. Koryta, *Electrochim. Acta*, **24**, 293 (1978).
3) M. Senda and T. Kakutani, *Hyomen*, **18**, 535 (1980).
4) C. Gavach and F. Henry, *J. Electroanal. Chem. Interfacial Electrochem.*, **54**, 361 (1974).
5) Z. Samec, V. Mareček, J. Koryta, and M. W. Khalil, *J. Electroanal. Chem. Interfacial Electrochem.*, **83**, 393 (1977).
6) Z. Samec, V. Mareček, and J. Weber, *J. Electroanal. Chem. Interfacial Electrochem.*, **100**, 841 (1979).
7) J. Koryta, P. Vaný́sek, and M. Březina, *J. Electroanal. Chem. Interfacial Electrochem.*, **67**, 263 (1976).
8) J. Koryta, P. Vaný́sek, and M. Březina, *J. Electroanal. Chem. Interfacial Electrochem.*, **75**, 211 (1977).
9) Z. Samec, V. Mareček, J. Weber, and D. Homolka, *J. Electroanal. Chem. Interfacial Electrochem.*, **99**, 385 (1979).
10) M. Senda, T. Kakutani, and T. Osakai, *Denki Kagaku*, **49**, 322 (1981).
11) P. Delahay, "New Instrumental Methods in Electrochemistry," Interscience, New York (1954), Chaps. 3, 6, and 8.
12) L. Q. Hung, *J. Electroanal. Chem. Interfacial Electrochem.*, **115**, 159 (1980).
13) J. Rais, *Collect. Czeck. Chem. Commun.*, **36**, 3253 (1971).
14) D. T. Sawyer and J. L. Roberts, "Experimental Electrochemistry for Chemists," Wiley, New York (1974), Chap. 5.